Bioactive Materials 10 (2022) 145–158

Contents lists available at ScienceDirect

Bioactive Materials

journal homepage: www.sciencedirect.com/journal/bioactive-materials

Exosome-loaded extracellular matrix-mimic hydrogel with anti-inflammatory property Facilitates/promotes growth plate injury repair

Pengfei Guan [a,1], Can Liu [c,1], Denghui Xie [d,1], Shichao Mao [a], Yuelun Ji [a], Yongchang Lin [a], Zheng Chen [f], Qiyou Wang [e,***], Lei Fan [b,**], Yongjian Sun [a,*]

[a] Department of Pediatric Orthopedic, Center for Orthopedic Surgery, The Third Affiliated Hospital of Southern Medical University, Guangzhou, 510515, China
[b] Department of Orthopedic Surgery, Nanfang Hospital, Southern Medical University, Guangzhou, 510515, China
[c] Department of Orthopedic Surgery, The First Affiliated Hospital, Zhejiang University School of Medicine, Hangzhou, 310003, China
[d] Department of Joint Surgery, Center for Orthopaedic Surgery, The Third Affiliated Hospital of Southern Medical University, Guangzhou, 510515, China
[e] Department of Orthopedics, The Third Affiliated Hospital of Southern Medical University, Guangzhou, Guangdong, 510515, China
[f] Department of Stomatology, The Third Affiliated Hospital of Sun Yat-sen University, Guangzhou, 510630, China

ARTICLE INFO

Keywords:
Extracellular matrix-mimic hydrogel
Exosomes
Immunomodulatory
Extracellular matrix deposition
Growth plate injury repair

ABSTRACT

Growth plate cartilage has limited self-repair ability, leading to poor bone bridge formation post-injury and ultimately limb growth defects in children. The current corrective surgeries are highly invasive, and outcomes can be unpredictable. Following growth plate injury, the direct loss of extracellular matrix (ECM) coupled with further ECM depletion due to the inhibitory effects of inflammation on the cartilage matrix protein greatly hinder chondrocyte regeneration. We designed an exosome (Exo) derived from bone marrow mesenchymal stem cells (BMSCs) loaded ECM-mimic hydrogel to promote cartilage repair by directly supplementing ECM and anti-inflammatory properties. Aldehyde-functionalized chondroitin sulfate (OCS) was introduced into gelatin methacryloyl (GM) to form GMOCS hydrogel. Our results uncovered that GMOCS hydrogel could significantly promote the synthesis of ECM due to the doping of OCS. In addition, the GMOCS-Exos hydrogel could further promote the anabolism of chondrocytes by inhibiting inflammation and ultimately promote growth plate injury repair through ECM remodeling.

1. Introduction

The growth plates in children are characterized by the cartilage area at the end of the long bone, responsible for longitudinal bone growth [1,2]. Unfortunately, they are quite vulnerable and account for 30% of all fractures in children [3]. Damage to growth plate cartilage usually leads to unwanted bony tissue repair, which may cause bone growth limitations in children and ultimately bring about differences in limbs length and angular deformities [4]. The current clinical treatment aims to remove excess bone bridges and using adipose tissue fillings to limit undesirable formations. However, patient outcomes can be unpredictable because factors such as the regeneration of the damaged cartilage and the state of the ECM (extracellular matrix) are often overlooked.

It is believed that the ECM microenvironment not only provides structural and mechanical support but also creates functional gradients by combining and isolating mitogens and morphogens, which are the main determinants of cell behavior [5]. In addition, a large number of spatiotemporal and mechanosensory signals from ECM regulate the development of chondrocytes -an essential element for growth plate cartilage, to perform biological functions [6]. The direct loss of a large amount of ECM after growth plate injuries and excessive inflammation can disrupt the ECM synthesis and decomposition balance. After an injury, an inflammatory response is triggered to regulate downstream remodeling and repair events [7]. These large number of inflammatory factors accelerate the degradation of ECM and stimulate the damaged chondrocytes to produce matrix metalloproteinases (MMPs), all while

Peer review under responsibility of KeAi Communications Co., Ltd.
* Corresponding author.
** Corresponding author.
*** Corresponding author.
E-mail addresses: wqiyou@163.com (Q. Wang), fanl1006@163.com (L. Fan), nysysyj@163.com (Y. Sun).
[1] The first three authors contributed equally to this work.

https://doi.org/10.1016/j.bioactmat.2021.09.010
Received 8 July 2021; Received in revised form 25 August 2021; Accepted 5 September 2021
Available online 16 September 2021

inhibiting the expression of cartilage matrix protein genes (SOX-9), further aggravating the catabolism of chondrocytes ECM [8].

Recent advances in three-dimensional (3D) polymer hydrogels have led to the development of materials with ECM motifs that can affect the self-renewal, differentiation, and migration of stem cell fate [9]. Gelatin methacryloyl (GM) hydrogels, similar to natural ECM in some properties, have decent biological properties and adjustable physical properties in a wide range of applications in tissue engineering, including bone, cartilage, and heart tissue engineering [10]. Chondroitin sulfate (CS) is a glycosaminoglycan (GAG) that exists primarily in the ECM of biological tissues and possesses chondrogenic properties [11]. Previous studies have shown that CS-based scaffolds not only exhibit good biocompatibility but also significantly induce the synthesis of cartilage matrix proteins, including COL-2 and Aggrecan by upregulating the cartilage specific-gene SOX-9 [12]. However, CS-based hydrogel can only be used as a timely supplement for ECM and cannot inhibit the degradation caused by inflammation after growth plate injury. Therefore, the importance of regulating the local immune microenvironment to minimize ECM degradation after injuries cannot be ignored.

Mesenchymal stem cells (MSCs) have been shown to have immunomodulatory properties and a repairing effect on tissues by regulating the immune microenvironment [13–15]. The anti-inflammatory effects of MSCs are attributed to their paracrine mechanisms, which mainly involve Exos secretion [16,17]. Exos are vesicles with a 30–200 nm diameter, similar to the parental MSC and are secreted by cells [18,19]. In addition, Exos are relatively easy to store and transport and many limitations related to cell transplantation can be avoided, including immunogenicity and tumorigenicity [20]. Exos carry various proteins, lipids, and a variety of non-coding RNAs, especially micro-RNAs, which play immunomodulatory roles by controlling the activity of recipient cells [21].

We surmised that combining ECM-like hydrogels with Exos derived from bone marrow mesenchymal stem cells (BMSCs) can promote ECM synthesis by providing ECM components and inhibiting inflammation, thereby promoting cartilage repair. To that end, we introduced doping aldehyde-functionalized chondroitin sulfate (OCS) into GM hydrogels to form biocompatible ECM (GMOCS) hydrogels by dynamic Schiff base bond formations. The dual network framework of GMOCS hydrogels ensured Exos sustained release to meet the growth plate repair requirement. The cell biocompatibility, adhesion, activity of the chondrocytes, and M1/M2 polarization of macrophage on the hydrogels were evaluated using an *in vitro* co-culture system. Furthermore, a growth plate injury model was established to study the role of the GMOCS-Exos in promoting immune microenvironment, chondrocytes regeneration, and ECM accumulation.

2. Materials and methods

2.1. Preparation of chondrocytes and RAW264.7 cells

Chondrocytes were obtained from the knee cartilage tissues of 2-week-old rats purchased from the Experimental Animal Center of Southern Medical University using an established method [22]. The gathered chondrocytes were cultured in Dulbecco modified Eagle medium (DMEM)/F-12 medium (Gibco) added with 10% FBS (Gibco), 100 U/mL penicillin and 100 U/mL streptomycin (Gibco) in 5% CO2 at 37 °C. The medium was changed every other day, and we used cells from the second passage to the fourth passage. RAW264.7 cells were cultured in a DMEM medium, including 10% FBS at 37 °C under 5% CO2 (ATCC cell bank).

2.2. Isolation, identification, and staining of exos derived from BMSCs

BMSCs were obtained by rinsing the bone marrow cavity of the tibias and femurs of 2-week-old rats, as described previously [23]. The collected cells were identified, and we selected those that met the characterization of BMSCs. BMSCs from the second to the sixth passage were cultured in low glucose DMEM (Gibco) supplemented with 10% Exo-free FBS (Gibco). After the cell fusion reached 50–60%, the supernatant was harvested for ultracentrifugation, according to a previous study [24]. Firstly, the supernatant was centrifuged at 300 g, 3000 g, and 10,000 g for 10 min to detach the Live/Dead cells and cell debris. Then, after centrifugation at 100,000 g for 90 min, the Exos at the bottom of the centrifuge tube were resuspended with phosphate-buffered saline (PBS) and stored at −80 °C. All the above centrifugal processes were carried out at 4 °C.

The collected Exos were identified by surface marker antibodies, including CD9 (ProteinTech) and TSG101 (Abcam). The morphology and size distribution were observed using transmission electron microscopy (TEM) and nanoparticle tracking analysis (qNano® system, Izon Science), respectively. The red fluorescent dye PKH26 (Sigma-Aldrich) was used for Exos staining according to the instructions.

2.3. Construction of exos-hydrogel system

2.3.1. Preparation of aldehyde-functionalized chondroitin sulfate (OCS)

The synthesis of OCS was done based on our previous research [25]. Briefly, 5 g CS was stirred in distilled water until completely dissolved (5% (w/v)), and 1.93 g of sodium periodate was added to the CS solution to react for 12 h in the dark. The solution was then placed in a dialysis bag (3500MW) and dialyzed in pure water below 50 °C for 24 h. The dialyzed solution was lyophilized in a freeze dryer for six days to finally obtain foamy aldehyde-functionalized chondroitin sulfate (OCS), which was stored at −20 °C.

2.3.2. Preparation of GM–OCS–exosomes (GMOCS-Exos) composite

GM freeze-dried powder was purchased from SunP Biotech. The GMOCS solution was prepared from GM solution (12.5%, w/v) in PBS containing the prepared OCS in a ratio of 2:1. After dissolving in a 70 °C water bath until there was no precipitation or dense foam, the solution was immediately sterilized with a 0.22 μm filter. According to the manufacturer's instructions, the GMOCS mixture solution, Exos, and photoinitiator 2-hydroxy-1- [4- (hydroxyethoxy) phenyl]-2-methyl-1-propanone (Irgacure 2959, 0.5% w/v) were added to the centrifugation tube and swirled for 3 min to ensure the uniform distribution of Exos in the solution. The hydrogel-Exos (GMOCS-Exos) were obtained by crosslinking for 10 s under ultraviolet radiation (6.9 mW/cm2, 360–480 nm).

2.4. Material characterization

The degree of oxidation (DO) of oxidized CS was evaluated by iodometric titration as described previously [25]. The molecular weights (MW) of GM and OCS were analyzed using Agilent PL-GPC50/Agilent 1260 and weight-average MW. The internal morphology and structure of the hydrogel were observed using field emission scanning electron microscopy (FE-SEM, ZEISS). The chemical composition of the hydrogel was analyzed using a Fourier transform infrared spectrometer (FTIR, Nicolet 6700, Thermo Fisher). In addition, the storage modulus (G′) and loss modulus (G″) of the GMOCS hydrogel was measured by rheological test (Physica MCR301, Anton Paar), and its dynamic oscillation frequency (10–0.1 Hz) was carried out at a fixed strain (5%). The compressive strength of the hydrogel was obtained from the DMA test (DMA, Q800, TA Instruments, USA) to allow the calculation of the hydrogel's strain-stress curve.

2.5. In vitro studies

2.5.1. Exos release profile

Cumulative and daily release profiles were assessed by a bicinchoninic acid (BCA) reagent test kit (Beyotime) according to the previous research [26]. To evaluate the release profile of the Exo from the

GMOCS, 200 μg of Exos and 60 μl of GMOCS hydrogel were mixed thoroughly to obtain GMOCS-Exos hydrogel. The GMOCS-Exos prepared above were incubated at 37 °C in PBS. The supernatant was collected on days 1, 3, 7, and 14 for free Exos detection using BCA.

2.5.2. Uptake of exos

To confirm that Exos contained in hydrogels could be phagocyted by cells, chondrocytes and RAW264.7 cells were co-cultured with GMOCS-Exos for 24 h. After 24 h, the culture medium was removed and washed three times with PBS and then fixed in 4% paraformaldehyde for 20 min. The phagocytosis of Exos was observed after Immunofluorescence (IF) staining under a laser confocal microscope (Leica) (cytoskeleton was stained with Actin-Tracker Green (Beyotime) and the nucleus was stained with Hoechst 33,342 (Beyotime)).

2.5.3. In vitro biocompatibility assessment

In vitro biocompatibility was performed and included cell viability, proliferation and adhesion experiments. To carry out the Live/Dead staining test, Chondrocytes with a density of 1 × 106 were seeded into 12-well culture plates and co-incubated with samples from each group for 24 h. The Live/Dead solution was then prepared in the ratio of 1 ml: 3 μl: 5 μl (PBS: calcein-AM(Invitrogen): PI(Invitrogen)) and added in each group and incubation was done for 30 min at 37 °C. After 1 × 10^6 chondrocytes were co-cultured with each group of samples for 1, 3, and 7 days, 100 μl/ml CCK-8 solution (Beyotime) was added to each well and incubated for 2 h. Then 100 μl supernatant was added onto a 96-well plate and the absorbance was measured at 450 nm with a microplate analyzer (BioTech). The adhesion of cells to the hydrogel was tested using the following method:

Briefly, cells with a density of 1 × 10^5 per well were cultured for three days, fixed with 4% paraformaldehyde, stained with Actin-Tracker Green and Hoechst, and the morphology of the cells was determined using a confocal microscope (Leica).

2.5.4. Establishment of GMOCS-Exos/RAW264.7 cells/Chondrocytes co-culture system

To detect the influence of the system's immune microenvironment on the chondrocytes, GMOCS-Exos/RAW264.7 cells/chondrocytes co-culture system was established in a Transwell chamber (Thermo-Fisher). The chondrocytes were handled with IL-1β (10 ng/ml) for 24 h before the experiment. As shown in Fig. 4A, GMOCS-Exos was co-cultured with 1 × 105 RAW264.7 cells and placed in the lower compartment, and 1 × 104 chondrocytes were placed in the upper compartment. A 1.0 μm pore size polycarbonate membrane separated the two layers without affecting the free passage of cytokines.

2.5.5. Gene expression

Total cellular RNA was extracted using an RNA extraction Kit (Omega) and then reverse-transcripted into cDNA using an EVO-MLV RT Kit (Accurate Biotechnology). LightCycler 480 SYBR Green Master Mix (TaKaRa) was used for qRT-PCR analysis. The endogenous control used the reference gene GAPDH. The relative gene expression was measured by the 2-ΔΔCt method. Three independent experiments were performed. The primers sequences in this study are listed in Table 1.

Table 2
Related information about primary antibodies.

Product Name	Species Reactivity	Dilution (cell/tissue)	Molecular weight	Source
GAPDH	Rabbit	1:1000	37 kDa	CST, America
Arg-1	Rabbit	1:1000/1:200	35 kDa	GeneTex, America
iNOS	Rabbit	1:1000/1:200	131 kDa	GeneTex, America
P65	Rabbit	1:1000	65 kDa	CST, America
p-P65	Rabbit	1:1000	65 kDa	CST, America
IKBα	Mouse	1:1000	40 kDa	CST, America
p-IKBα	Rabbit	1:1000	40 kDa	CST, America
COL-2	Rabbit	1:1000/1:200	142 kDa	Abcam, England
SOX-9	Rabbit	1:1000	56 kDa	Abcam, England
CD9	Rabbit	1:1000	25 kDa	Proteintech, America
MMP-13	Rabbit	1:1000/1:200	54 kDa	Abcam, England
TSG101	Rabbit	1:1000	46 kDa	Abcam, England

2.5.6. Immunofluorescence

Samples were fixed with 4% paraformaldehyde in PBS for 30 min. Then, the cells or tissues were treated with 0.2% Triton X-100 (Biofroxx) for 10min and blocked with 3% bovine serum albumin (BSA, Biofroxx) for 1 h at room temperature. The samples were incubated overnight at 4 °C in primary antibodies. Hereafter, the sample was washed three times with PBS and incubated with the secondary antibody for 2 h at room temperature, and Hoechst (Beyotime) staining was performed. The antibodies are listed in Table 2. Finally, the staining was observed under a confocal microscope (Leica).

2.5.7. Western Blot

Cells were grounded into a homogenate in RIPA buffer (CWBIO) containing protease and phosphatase inhibitors (Thermo Fisher). The supernatants were lysed in ice for 30 min and collected by centrifuging at 12,000 rpm at 4 °C for 30 min. The total protein concentration was determined with the BCA kit (Beyotime). The supernatants were mixed with loading buffer (Beyotime), and equal amounts (40 μg) of protein were loaded onto sodium dodecyl sulfate-polyacrylamide gel electrophoresis (SDS-PAGE). After the separated protein was transferred to the polyvinylidene difluoride (PVDF, Thermo Fisher) membrane, the PVDF membrane was blocked with 5% skim milk for 1 h and then incubated with the primary antibodies (Table 2) overnight. The PVDF membrane was then incubated with the secondary antibody for 1 h before applying the enhanced chemiluminescence (ECL) kit (Thermo Fisher) for visualization. Tris Buffered Saline with Tween® 20(TBST) was used to wash the membranes thrice before each step. The results were analyzed using ImageJ software.

2.6. In vivo studies

2.6.1. Ethics statement

Animal experiments were approved by the Animal Experimentation Ethics Committee of Southern Medical University. All experimental procedures on animals were carried out in accordance with the

Table 1
Primer sequences of each gene.

Target	Forward	Reverse
COL-2	AACCCAAAGGACCCAAATAC	CCGGACTGTGAGGTTAGGAT
SOX-9	CGTGGTGACAAGGGTGAGAC	TAGGTGATGTTCTGGGAGGC
MMP-13	AGGCCTTCAGAAAAGCCTTC	GAGCTGCTTGTCCAGGTTTC
Arg-1	CTCCAAGCCAAAGTCCTTAGAG	GGAGCTGTCATTAGGGACATCA
IL-10	CTTACTGACTGGCATGAGGATCA	GCAGCTCTAGGAGCATGTGG
iNOS	GTTCTCAGCCCAACAATACAAGA	GTGGACGGGTCGATGTCAC
TNF-α	CGAGTGACAAGCCTGTAGCC	ACAAGGTACAACCCATCGGC
GAPDH	AGCCCAGAACATCATCCCTG	CACCACCTTCTTGATGTCATC

Guidelines for the Care and Use of Laboratory Animals of the National Institutes of Health.

2.6.2. Rat drill-hole growth plate injury

To study the role of GMOCS-Exos in the process of growth plate injury repair, 6-week-old male Sprague Dawley (SD) rats were used to establish the distal femoral drill-hole growth plate injury model, as described previously [27]. In brief, after exposure to the distal femoral trochlear groove, a central defect of approximately 2.0 mm was created at the distal femur by drilling the articular cartilage between the condyles using a 15 G needle. A mixture of around 15 μl GMOCS-Exos was injected into the defect site and rapidly crosslinked in situ under UV irradiation. A total of 18 SD rats were randomly divided into three groups: growth plate injury group (control, n = 6), pure hydrogel group (GMOCS, n = 6), and Exo-loaded hydrogel group (GMOCS- Exos, n = 6). All rats were sacrificed after 8 weeks postoperatively.

2.6.3. Hemolysis test and degradation study

Whole rat blood and hydrogel were incubated at 37 °C for 4 h to study the hemolytic changes. PBS and Triton X-100 (Biofroxx) were used as the negative control and positive control, respectively. After incubation, whole rat blood was centrifuged at 10,000 g for 5 min at 4 °C. The OD value of the supernatant was determined by measuring the absorbance at 540 nm using an ultraviolet–visible spectrometer. The following formula was used to calculate the percentage of red blood cell hemolysis, as previously described [28]: RBC hemolysis = 100% × $(OD_{sample} - OD_{PBS})/(OD_{triton} - OD_{PBS})$.

To simulate the in-situ degradation culture conditions, GMOCS hydrogels (n = 3) were placed in 5 ml PBS and incubated at 37 °C. The weight of the hydrogel was measured at different time points after removing excess water with filter paper. The hydrogel degradation was calculated by dividing the weight of the final hydrogel by the initial hydrogel.

2.6.4. Micro-computed tomography (Micro-CT)

After 8 weeks, all rats were killed using carbon dioxide asphyxiation and their femurs were removed for further analysis. The restoration of the rat growth plate was assessed using a VivaCT 40 system (Scanco Medical, Switzerland) as previously described [27]. Bone bridge formation in each group was determined by comparing the amount of bone volume infiltration in a specific size area. As shown in Fig. 6A, a 2 mm × 15 slice (0.32 mm) cylindrical area containing the drill-hole injury was selected to compare bone bridge formation in each group. After that, bone volume fraction (BVF), trabecular number (Tb·N), and trabecular thickness (Tb·Th) were used to measure bone bridge formation.

2.6.5. Histological analysis and immunohistochemistry

The rats were sacrificed and whole femurs were collected after 8 weeks of treatment. Samples were fixed in 4% paraformaldehyde (pH 7.5) for 1 day and decalcified in decalcifying solution for 21 days, the samples were then embedded in paraffin and cut into 5 μm sections. Sagittal sections from the growth plate defect were stained with hematoxylin, and eosin (HE, saffron O/Fast Green (SO, ServiceBio), and immunohistochemical staining. The rabbit anti-COL-2 (Abcam), MMP-13 (Abcam), Arg-1 (Gentex), and iNOS (Gentex) primary antibodies (Table 2) were used for immunohistochemistry.

2.7. Statistical analysis

GraphPad Prism 5 software and SPSS version v19.0.0 (IBM, USA) were used for nonparametric Kruskal-Wallis test or one-way analysis of variance (ANOVA) with Tukey's test. The experimental data were expressed as mean ± standard deviation (Mean ± SD). All experiments were repeated at least three times. $P < 0.05$ is considered statistically different.

3. Results and discussion

3.1. Characterization of BMSCs-Exos

To confirm the isolation of BMSCs-derived Exos obtained from rat's bone marrow, micrographs were obtained through TEM, which showed a round or elliptical morphology with complete cell membrane structure (Fig. S1A). Additionally, the qNano® system was used for quantification and size profiling. The particle size distribution was found to be mainly around 100 nm, consistent with that of exosomal dimension (Fig. S1B). Furthermore, Western blotting analysis showed that the nanoparticles expressed the exosomal specific markers CD9 and TSG101 (Fig. S1C). Hence, the above results confirm that the Exosomes were successfully isolated from BMSCs.

3.2. Synthesis and characterization of materials

A mixture of GMOCS and Exos crosslinked by a photoinitiator under UV irradiation was prepared (Fig. 1A). The general view of GMOCS-Exos hydrogel was shown in Fig. 1B, indicating that we successfully transformed the GMOCS-Exos mixture solution into a GMOCS-Exos hydrogel. With sodium periodate as the oxidant, the hydroxyl group on the CS polysaccharide skeleton was partially oxidized to form an aldehyde group. The FTIR analysis confirmed the successful synthesis of OCS with a new peak at 1725 cm^{-1} that appeared in the OCS spectrum compared to CS. We also successfully introduced the aldehyde group, as shown in Fig. 1C [25]. The DO of OCS measured by iodometric titration was 86.73 ± 0.72. Moreover, the results of GPC showed that the molecular weights of GM and OCS were 210 kDa and 27 kDa, respectively (Table S1). The free amino group in the GM hydrogel skeleton could form a Schiff base bond with the aldehyde group in OCS to allow reversible covalent cross-linking. Rheological properties tests demonstrated that the storage modulus (G′) of GMOCS and GMOCS-Exos was much greater than the loss modulus (G″), which indicated that they were both stable viscoelastic solids [29]. In addition, the average storage modulus of GMOCS was 2351 ± 20 Pa, and that of GMOCS-Exos was 2267 ± 50 Pa, showing no significant difference. This indicates that the addition of Exos did not change the mechanical properties of GMOCS hydrogel (Fig. 1D). Besides, the strain-stress curve of the GMOCS hydrogel shows that the compressive strength value of the hydrogel when the strain reaches 88% was 0.25 MPa (Fig. S2), which satisfied the compressive strength value of human cancellous bone (0.15–13.7 MPa) [30]. SEM imaging showed that the hydrogels presented a porous network structure and that the Exos were bound to the inner surface of the GMOCS hydrogel (Fig. 1E). Immunofluorescence imaging further revealed the 3D spatial distribution of Exos in the hydrogel (Fig. 1F). Together, these results indicate that Exos were successfully loaded onto the GMOCS hydrogel. More importantly, we showed that Exos release was continuous for 14 days, and more than 80% of the unobstructed loaded Exos were released from the GMOCS hydrogel, ensuring an optimal biological effect on the growth plate (Fig. 1G–H).

3.3. In vitro biocompatibility of each group

The growth plate is essentially made up of hyaline cartilage [31]. Therefore, investigating the biocompatibility of our GMOCS-Exos hydrogel is an important prerequisite for the treatment of growth plate injury. Live/Dead staining showed that a large number of live cells (green) and very few dead cells (red) were observed in each group (Fig. 2A). The results of the CCK-8 analysis further showed that chondrocyte proliferation increased with culture time. Moreover, the cell activity of chondrocytes in the GMOCS-Exos and Exos groups was significantly higher than the GM group on the 3rd and 7th days, indicating that OCS and Exos had outstanding biological activity for chondrocyte proliferation (Fig. 2B). CS, is a natural GAG (glycosaminoglycans) present in cartilage and participates in many

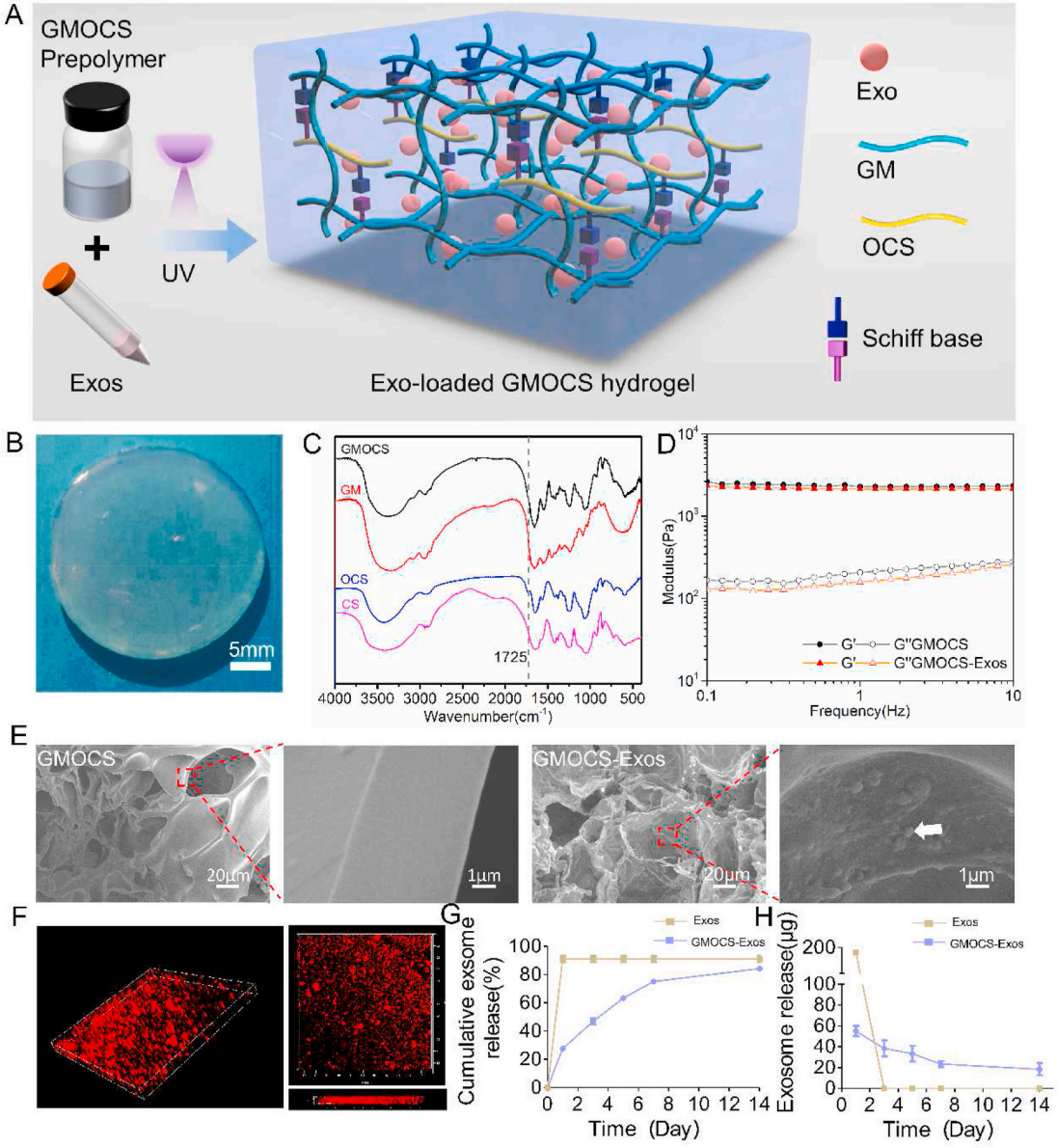

Fig. 1. Characteristics of GMOCS hydrogel loaded with Exos. (A) Schematic representation of the synthesis and chemical structure of GMOCS hydrogel. (B) A photograph of the GMOCS-Exos hydrogel. (C) FTIR spectra of GM, CS, OCS, and GMOCS. (D) Rheological analysis of GMOCS hydrogel with or without Exos. (E) SEM image of GMOCS hydrogel with or without Exos. The white arrow represents Exos loaded on the hydrogel. (F) 3D image of Exos labeled with PKH26 in GMOCS hydrogel. (G) The cumulative release profile of Exos with or without GMOCS hydrogel for 14 days (n = 3). (H) The daily release curve of Exos with or without GMOCS hydrogel (n = 3).

signal transduction pathways of chondrocytes and has been shown to promote chondrocyte proliferation and regeneration [32]. Studies have also shown that Exos from MSCs can promote cell migration and proliferation and reduce apoptosis through AKT and ERK signaling pathways [33]. Cytoskeleton imaging revealed that the chondrocytes in each group had a better expansion area and length, further indicating that the GMOCS-Exos had good affinity and adhesion for chondrocytes (Fig. 2C).

3.4. GMOCS-exos promote the polarization of RAW264.7 cells through the NF-κB pathway

After an injury, the growth plate's inflammatory response disrupts chondrocytes' anabolic and catabolic balance, thereby degrading the ECM by matrix-degrading enzymes [31]. Since macrophages are the primary mediators of inflammation after injury, we studied the polarization effect of Exo-loaded hydrogel on RAW264.7 cells *in vitro*. RAW264.7 cells handled with LPS (500 ng/ml) were cultured on each group of hydrogel samples for 3 and 7 days to verify the immunomodulatory properties of GMOCS-Exos hydrogel. The expression of related inflammatory molecules was detected by qPCR, Immunofluorescence and Western Blot assay. As shown in Fig. 3A, the Exos loaded on the GMOCS hydrogel were able to be phagocytosed by RAW264.7 cells to exert an immunomodulatory effect. On day 3, the qPCR results showed that the expression values of M2 phenotypic markers (Arg-1 and IL-10) in GMOCS-Exos and Exos groups were significantly higher than those in the control group. However, there was no significant difference between the GMOCS group and the control group, indicating that GMOCS had no notable effect on macrophages, while Exos loaded in hydrogels significantly promoted the M2 polarization of macrophages (Fig. 3B). Moreover, on day 7, the qPCR results showed that GMOCS-Exos hydrogel significantly increased the expression levels of Arg-1 and IL-10, while that of iNOS and TNF-α decreased. This effect can be attributed to the

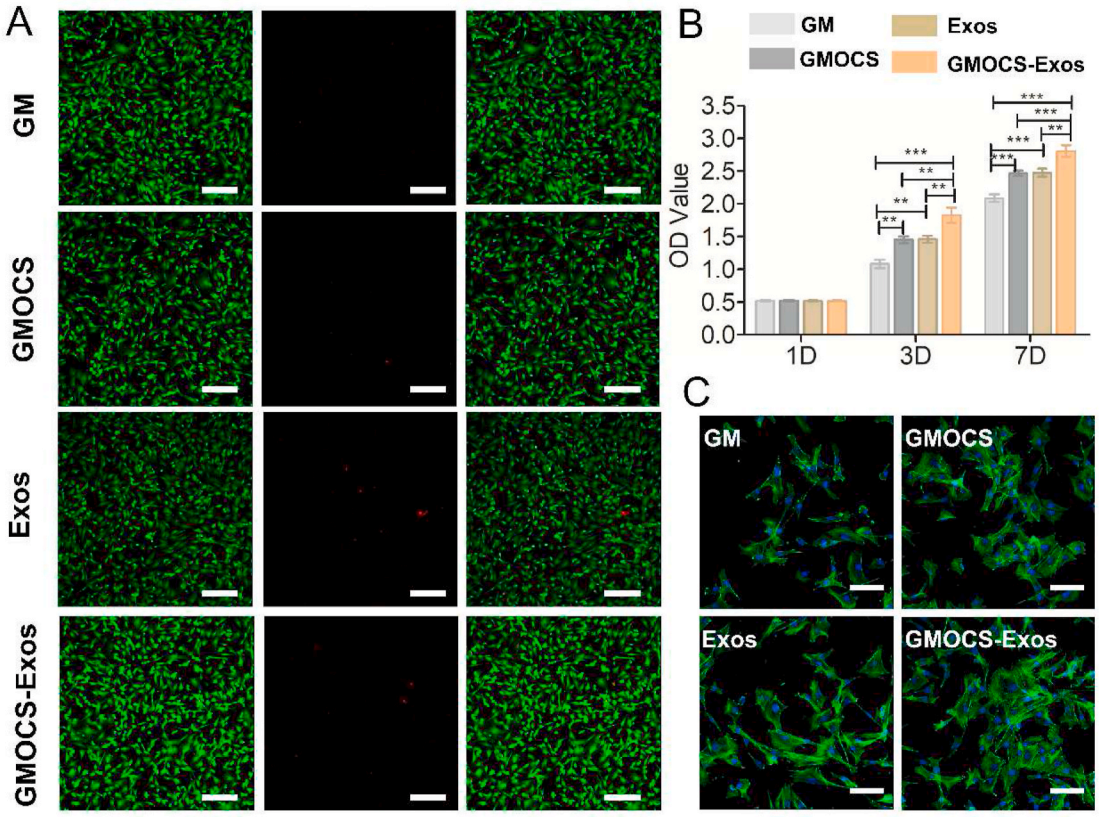

Fig. 2. Biocompatibility evaluation of each group. (A) Live/Dead analysis for each group after 1 day of cell culture. The cells marked in green (stained by AM) and red (stained by PI) represent live and dead cells, respectively. Scale bar = 200 μm. (B) The CCK-8 assay was measured in each group after 1, 3 and 7 days of cell culture (n = 5). (C) The cytoskeleton images showed the adhesion of chondrocytes after 3 days of culture in each group. Scale bar = 100 μm. ANOVA followed by Tukey's test was used for statistical analysis (*p < 0.05, **p < 0.01, and ***p < 0.001).

sustained release of Exos from the GMOCS-Exos hydrogel, which was shown to promote the long-term polarization of immune cells [34]. Consistent with our qPCR analysis, the proportion of iNOS positive cells was lower in the GMOCS-Exos group compared to the control group, while the proportion of Arg-1 positive cells was higher (Fig. 3C–D). Western Blot analysis further confirmed that GMOCS-Exos significantly down-regulated iNOS protein and up-regulated Arg-1 protein (Fig. 3E–F). Together, our results indicate that Exos had a strong immunomodulatory effect by promoting macrophage M2 polarization. Exos are small nanoscale vesicles that contain nucleic acid, protein, and other components, which play a biological role mainly by the extracellular release of active components to carry out cell communication and conduction [35]. Numerous studies have confirmed that MSC-derived Exos are rich in molecules that can regulate immunity, including mRNA, miRNA, cytokines, and chemokines, which play an important role in regulating the phenotype and function of immune cells [36]. According to our previous studies, Exos derived from BMSCs contain biologically active molecules, especially miR-199a, which can regulate immunity by inhibiting the NF-κB pathway [23]. Our results further revealed that the expression of *p*-IKBα and downstream factor p-P65 was significantly down-regulated in the GMOCS-Exos group and Exos group, consistent with previous findings. More importantly, we showed that GMOCS-Exos enhanced the polarization of macrophages from M1 to M2 by inhibiting the NF-κB signaling pathway, which could be beneficial for growth plate repair (Fig. 3G–H).

3.5. GMOCS-exos facilitate the repair of IL-1β damaged chondrocytes by improving the immune microenvironment

To verify the impact of the improved immune microenvironment on chondrocytes, a sample/RAW264.7 cells/chondrocyte co-culture system was constructed (Fig. 4A). The chondrocytes were treated with IL-1β before the experiment, as described previously [37]. After 3 and 7 days of co-cultivation, immunofluorescence staining, qPCR, and Western Blot were used to evaluate the ECM regeneration of chondrocytes. As shown in Fig. 4B, there was no significant difference in the GMOCS group compared to the control group at co-culture day 3 or day 7. Interestingly, the GMOCS-Exos group and the Exos group significantly upregulated COL-2 and SOX-9 levels of the injured chondrocytes but down-regulated the expression of MMP-13, showing that GMOCS-Exos and Exos can promote IL-1β-induced-chondrocytes repair (Fig. 4B). The qPCR results showed no significant difference between the Exos group and the GMOCS-Exos group on the third day; however, the therapeutic effect of the GMOCS-Exo group was significantly better than that of the Exos group on the seventh day, due to its sustained-release effect and ability to provide an anti-inflammatory environment (Fig. 4B). SOX-9 is considered one of the key transcription factors for cartilage formation and can regulate the expression of chondrogenesis-related markers (type II collagen) and the formation of the GAG matrix [38]. Proinflammatory factors, including TNF-α and IL-1β released by M1 macrophages, can firmly restrain the expression of the chondrogenic extracellular matrix (ECM) protein gene by reducing the level of chondrogenic transcription factor SOX9 mRNA in inflammatory environments. Exos can alleviate the inhibitory effect of inflammation on chondrocytes by regulating the M2 polarization of macrophages, therefore promoting the synthesis of ECM. Our Western Blot and Immunofluorescence staining analyses were consistent with qPCR results at co-culture day 7, showing the highest expression of COL-2 protein and the lowest expression of MMP-13 protein when treated with GMOCS-Exos (Fig. 4C–F). In addition, to further confirm the effect on RAW264.7 cells, we performed Western Blot

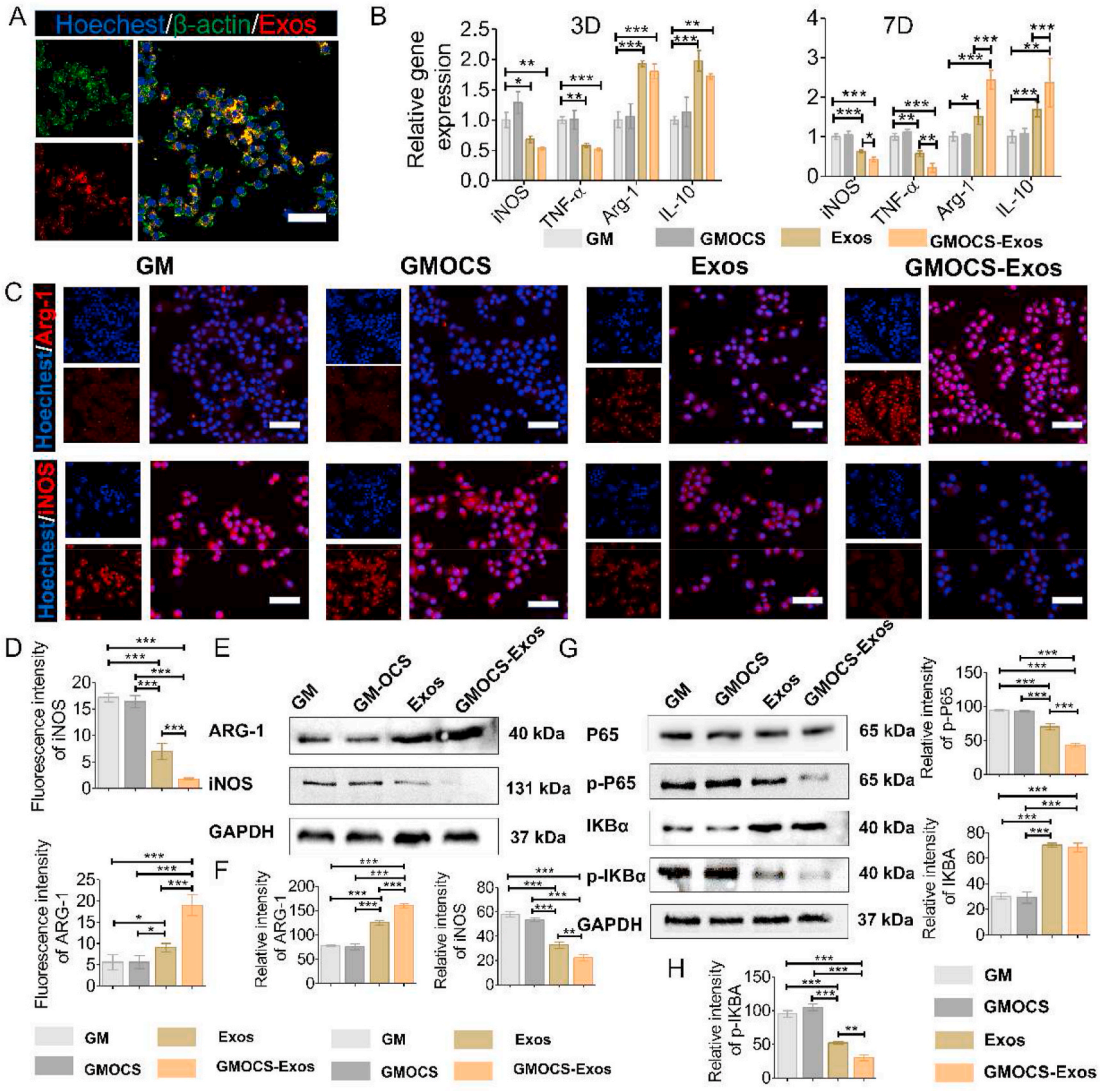

Fig. 3. GMOCS hydrogel loading Exos promote the polarization of RAW264.7 cells through the NF-κB pathway. (A) Cytoskeleton staining imaging shows PKH26 labeled Exos loaded on the hydrogel taken up by RAW264.7 cells. Scale bar = 50 μm. (B) mRNA expression of anti-inflammatory cytokines (Arg-1, IL-10) and pro-inflammatory cytokines (iNOS, TNF-α) in each group (n = 3). (C) Immunofluorescence of the RAW264.7 cells in each group for the Arg-1 and iNOS (red). Scale bar = 50 μm. (D) Quantitative analysis of the fluorescence intensity of iNOS and Arg-1 in each group (n = 3). (E) Western Blot analysis of the Arg-1 and iNOS protein bands in each group. (F) Quantitative analysis of the Arg-1 and iNOS protein expression in each group (n = 3). (G) Western Blot analysis of the IKBα, p- IKBα, P65 and p-P65 protein bands in each group. (H) Quantitative analysis of the IKBα, p- IKBα, p-P65 protein expression in each group (n = 3). ANOVA followed by Tukey's test was used for statistical analysis (*$p < 0.05$, **$p < 0.01$, and ***$p < 0.001$).

analysis after 7 days of co-culture with GMOCS-Exos/chondrocytes in the presence or absence of RAW 264.7 cells. The results showed that in the absence of RAW264.7 cells, the chondrogenic effect of GMOCS-Exos was significantly reduced (Fig. S3). Together our findings indicate that Exos sustained-release in the hydrogel could provide a proper chondrogenesis immune microenvironment by inhibiting inflammation, thereby enhancing the synthesis of chondrocyte ECM.

3.6. GMOCS-exos promote the repair of IL-1β damaged chondrocytes

To evaluate the direct chondrogenesis effect of GMOCS-Exos hydrogel, chondrocytes pretreated with IL-1β were cultured directly on the samples for 7 days (Fig. 5A). The cytoskeleton staining images showed that the Exos loaded on GMOCS hydrogel were released and taken up by chondrocytes after 24 h of co-culture (Fig. 5B). The qPCR results demonstrated that the expression of chondrogenic genes, SOX-9 and COL-2 in the GMOCS group were significantly higher than those in the control group, indicating that the doping of OCS significantly contributed to the repair of chondrocytes (Fig. 5C). CS has been shown to promote cartilage formation by binding to integrins, which in turn increased the expression of TGF-1, leading to the production of hyaluronic acid and COL-2 [39]. We further found that the expression level of SOX-9 and COL-2 genes in the Exos and GMOCS-Exos groups were significantly higher in comparison to the control group, with the highest level found in the GMOCS-Exos group, suggesting that Exos can alleviate IL-1 damage to chondrocytes and that GMOCS hydrogel combined with Exos can further promote repair of damaged chondrocytes. The non-coding RNAs in Exos, such as miR-23 b and miR-92a, play a vital role in regulating the proliferation, chondrogenesis, and matrix synthesis of chondrocytes through the MAPK, AKT, and ERK pathways [40]. IF and Western Blot results showed that COL-2 expression in the GMOCS-Exos group was 4.2 ± 0.3 and 3.7 ± 0.5 times higher than that of the control group, consistent with qPCR results (Fig. 5D–G). Moreover, we found that GMOCS-Exos hydrogel can produce a direct synergistic regulation effect on chondrogenesis. Together, we showed that GMOCS-Exos could exert both an immunomodulatory effect and a

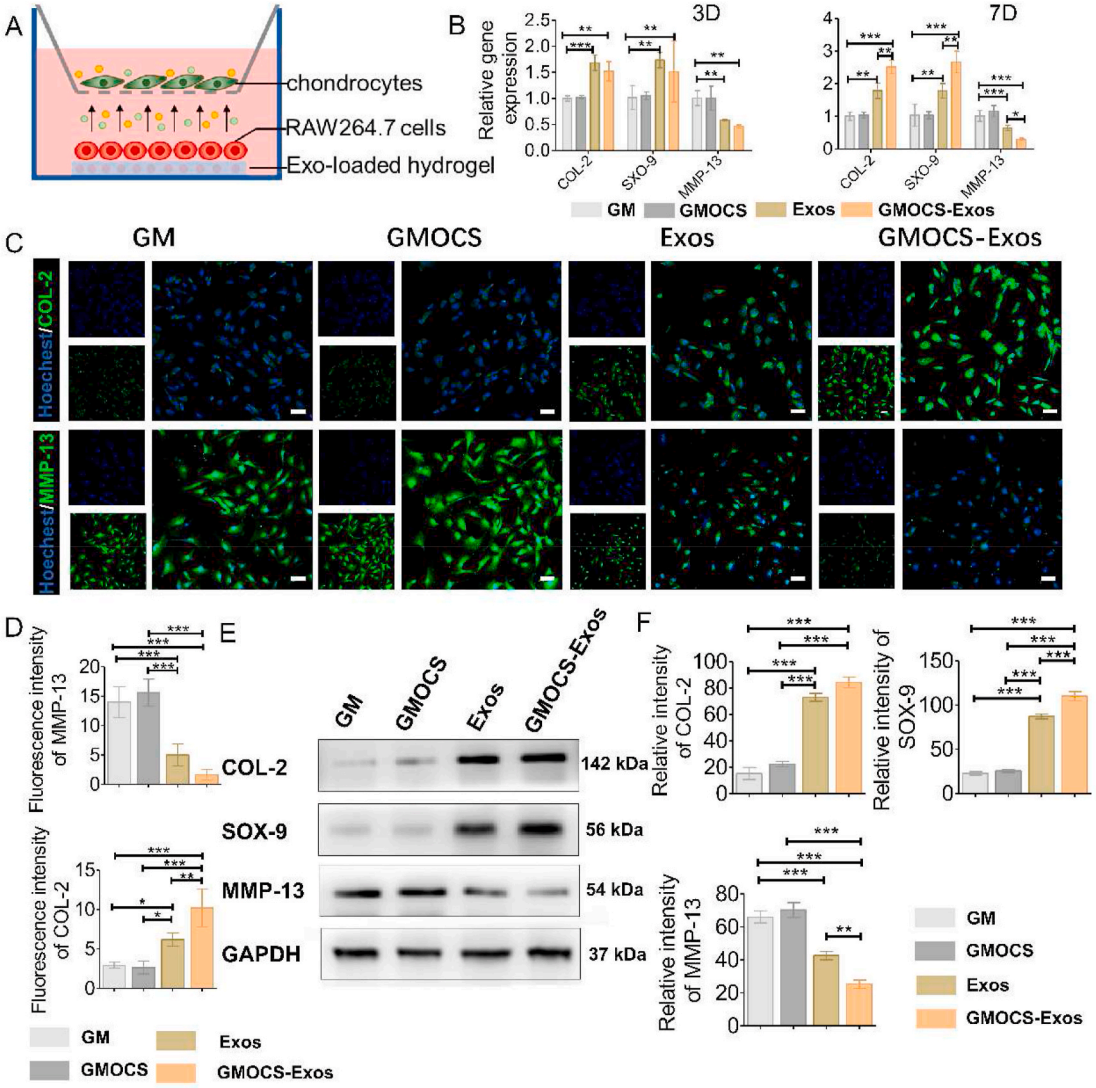

Fig. 4. The effect of macrophage polarization on damaged chondrocytes. (A) Construction of a co-culture model of RAW264.7 cells/IL-1β damaged chondrocytes. (B) qPCR determined mRNA levels of MMP-13, COL-2, and SOX-9 (n = 3). (C) Immunofluorescence staining of COL-2 and MMP-13. Scale bar = 50 μm. (D) Quantitative analysis of the fluorescence intensity of COL-2 and MMP-13 (n = 3). (E) Western Blot analysis of the MMP-13, COL-2, and SOX-9 protein expression in each group. (F) Quantitative analysis of the MMP-13, COL-2, and SOX-9 protein expression in each group (n = 3). ANOVA followed by Tukey's test was used for statistical analysis (*$p < 0.05$, **$p < 0.01$, and ***$p < 0.001$).

direct chondroprotective effect to synergically promote chondrogenesis.

3.7. GMOCS-exos boost repair of growth plates and reduce bone bridge formation after injury

The hemolysis test revealed that all the hydrogels exhibited high biocompatibility for repair applications (Fig. S4). Similar to the control group, the measured OD value of the hydrogel group was lower than 0.2, indicating that the GMOCS hydrogel would not cause significant hemolysis. In addition, the *in vitro* degradation test results showed that the hydrogel could be maintained for at least 2 weeks under physiological conditions, which ensured the sustained release and therapeutic effect of Exos (Fig. S5). The growth plate surgery process and the implantation of the hydrogel are shown in Fig. 6A. At 7 days after GMOCS-Exos transplantation, *in vivo* imaging of rats showed that the fluorescence signal of PKH26-labeled Exos could still be detected, indicating that the Exos worked locally around the injury site of the growth plate (Fig. S6). After 8 weeks post-injury, we assessed the bone bridge formation at the injury site by Micro-CT. The quantitative results showed that Bridge BVF, Tb·N and Tb·Th in the GMOCS group were significantly lower than the control group (Fig. 6D), indicating that the implantation of GMOCS hydrogel significantly reduced the formation of bone bridges at the injury site. In addition, compared with the ECM hydrogel implantation alone, the ECM scaffold loaded with Exos can significantly reduce the ingrowth of bone bridges at the injury site of the growth plate (Fig. 6C–D). H&E and Safranin O/Fast Green staining indicated little cartilage formation and more bone and mesenchymal tissue infiltration in the simple injury group, while prominent cartilage formation was seen in the defect area of the GMOCS-Exos group (Fig. 6E). There were almost no neogenetic chondrocytes at the injury site of the control group, while obvious chondrocytes and even the column structure of chondrocytes in the growth plate was restored in the GMOCS-Exos group (Fig. 6E). The growth plate comprises a resting zone, a proliferation zone, and a hypertrophic zone which possess essential biological functions [41]. During the growth plate development, chondrocytes go from a resting state to a hypertrophic state, followed by subsequent calcification and vascular invasion, accompanied by a series of temporal and spatial signal adjustments, eventually forming bone [42]. At present, the commonly used materials for growth plate injury include fat, physeal allograft, and iliac apophyseal autograft to prevent the formation of

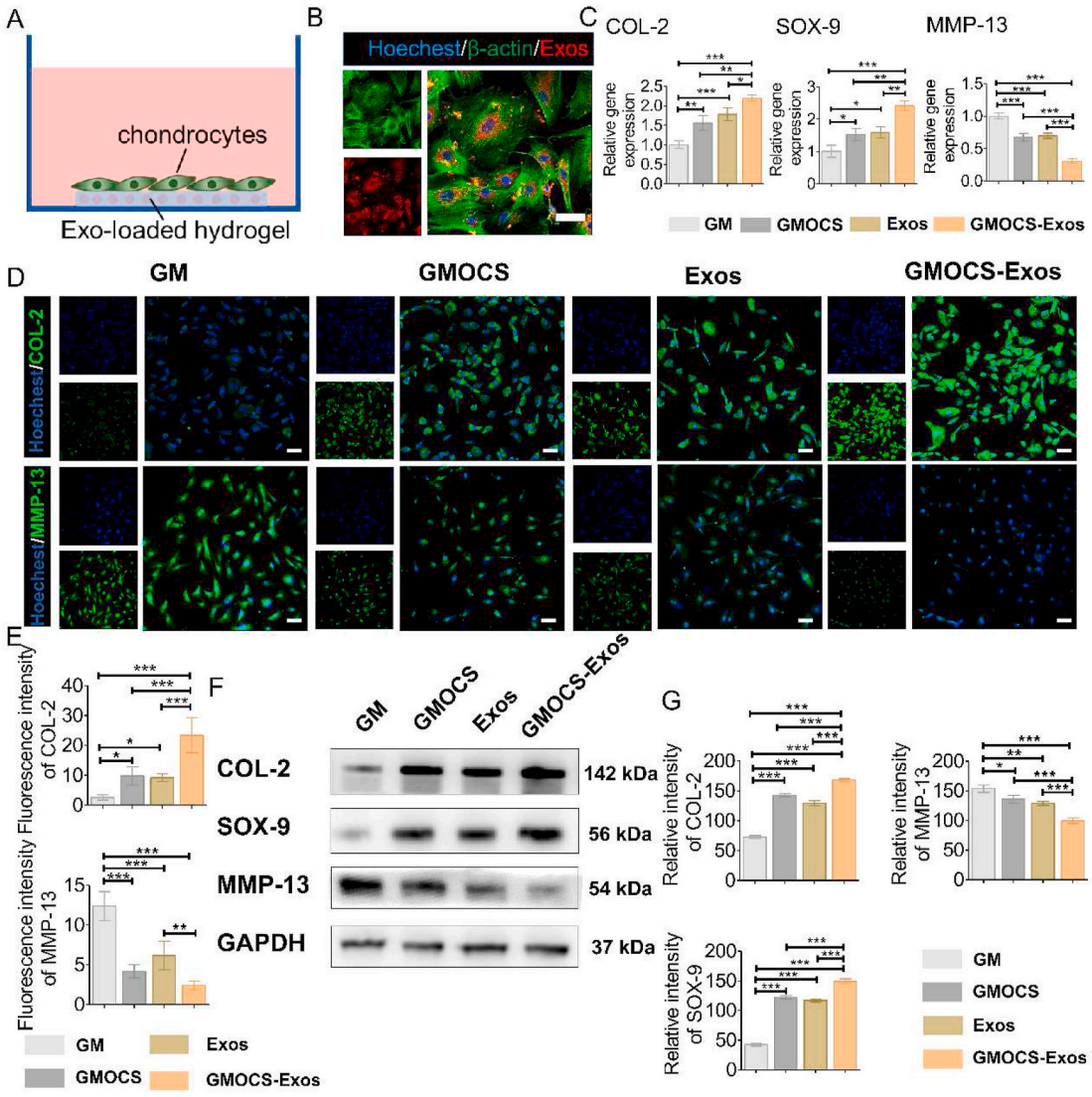

Fig. 5. GMOCS-Exos promote the repair of damaged cartilage cells. (A) Construction of a co-culture model of samples/IL-1β damaged chondrocytes. (B) Cytoskeleton staining images showing PKH26 labeled Exos loaded on the hydrogel taken up by chondrocytes. Scale bar = 50 μm. (C) qPCR determined mRNA levels of MMP-13, COL-2, and SOX-9 (n = 3). (D) Immunofluorescence staining intensity of COL-2 and MMP-13. Scale bar = 50 μm. (E) Quantitative analysis of the fluorescence intensity of COL-2 and MMP-13 (n = 3). (F) Western Blot analysis of the MMP-13, COL-2, and SOX-9 protein bands in each group. (G) Quantitative analysis of the MMP-13, COL-2, and SOX-9 protein expression in each group (n = 3). ANOVA followed by Tukey's test was used for statistical analysis (*$p < 0.05$, **$p < 0.01$, and ***$p < 0.001$).

bone bridges after the resection of the damaged part of the epiphysis. However, these materials can only prevent bone bridge formations at the growth plate defects to a certain degree and cannot regenerate or repair [43]. The implantation of our GMOCS hydrogel not only limited the growth of bone bridges but also promoted the growth of cartilage. Moreover, the local release of Exos can also facilitate cartilage regeneration and reduces bone bridge formation. The above results indicate that Exo-loaded GMOCS hydrogel significantly inhibits bony repair in the damaged part of the growth plate and instead promotes cartilage regeneration.

3.8. *GMOCS-exos regulate the polarization of macrophages at the injury site*

To confirm that GMOCS-Exos can regulate the inflammatory response after growth plate injury *in vivo*, macrophage phenotype polarization was detected in the injured area using the unique markers iNOS and Arg-1. There was almost no significant difference between the GMOCS and the control groups, indicating that hydrogel implantation alone had no modulating effect on local inflammation, similar to our *in vitro* study. Relative to the control and GMOCS groups, the expression of Arg-1 at the injury site in the GMOCS-Exos group was higher. In contrast, iNOS displayed significantly lower expression in the GMOCS-Exos than in the control and GMOCS groups. This could be explained by the ability of Exos to induce the transformation of macrophages from M1 to M2 at the injury site. Immune activity plays an essential role in tissue damage and repair, especially for chondrocytes. Inflammatory cytokines produced by pro-inflammatory immune cells, such as IL-1β, iNOS, and TNF-α, are rapidly up-regulated, leading to overexpression of matrix proteinases such as MMP-1 and MMP-13, further leading to apoptosis of chondrocytes and matrix degradation after cartilage injury [44]. M2 macrophages, also known as wound-repair macrophages, create an anti-inflammatory environment necessary for tissue repair and remodeling [45]. The immune microenvironment regulation we achieved was conducive to chondrocyte survival and cartilage regeneration. Previous studies have shown that injecting M2 macrophage activators into the joint cavity of animals with osteoarthritis can prevent the formation of osteophytes and slow down cartilage damage [46]. Our

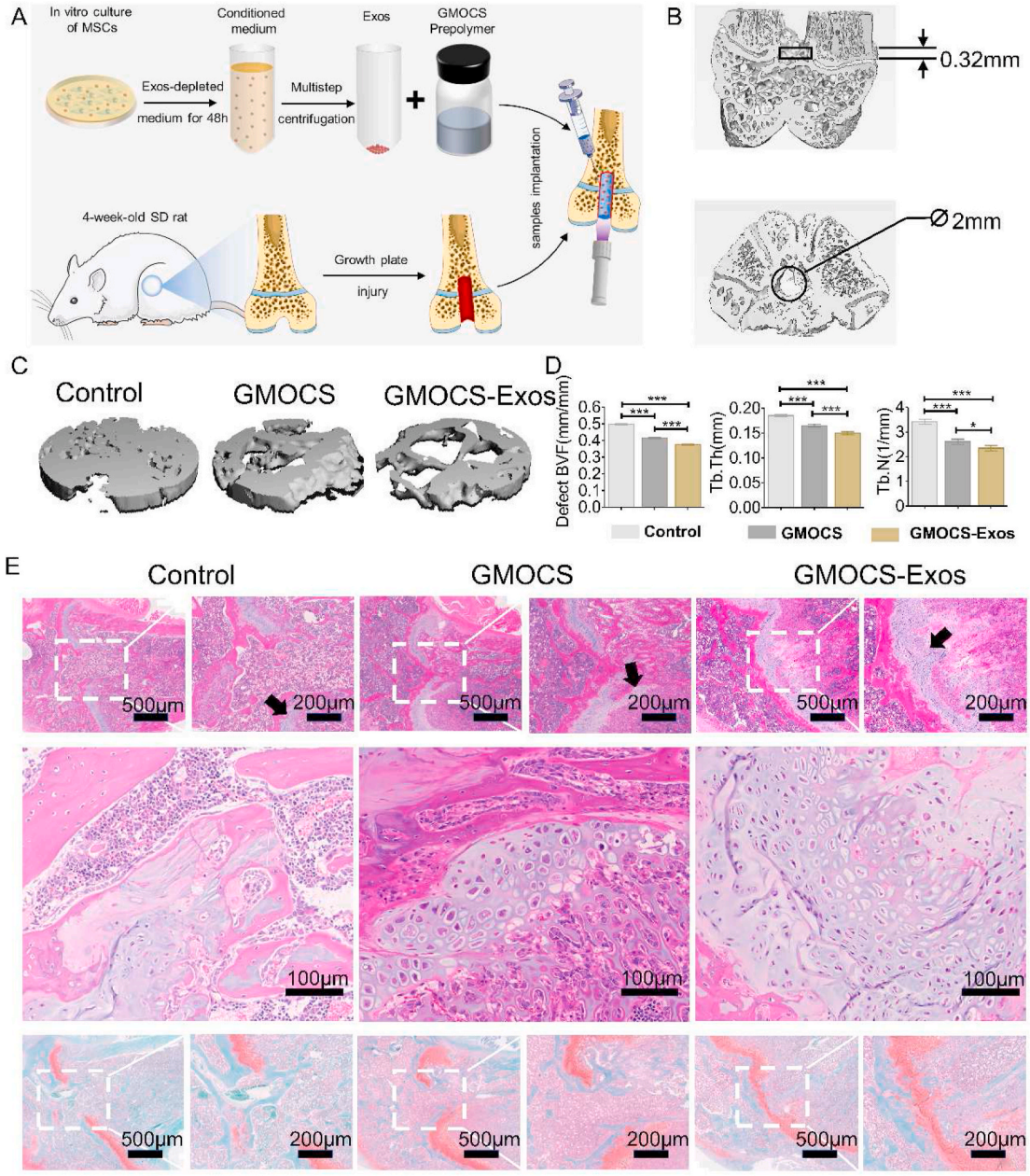

Fig. 6. GMOCS-Exos stimulate the repair of growth plates after injury and diminishes bone bridge formation. (A) Illustration of the surgical procedure performed on the rat femur drill model. (B) Measurement of the mineral content within the defect. (C) Micro-CT images of bone bridge formation in the defect. (D) Quantitative measurement of bone bridge formation at the defect site (n = 3). (E) Images of H&E and Safranin O/Fast Green staining of the defect site. The black arrow indicates the area of regenerated cartilage and is enlarged below it. ANOVA followed by Tukey's test was used for statistical analysis (*p < 0.05, **p < 0.01, and ***p < 0.001).

research found that GMOCS-Exos induced higher expression of anti-inflammatory factors at the injury site, accompanied by a pro-chondrogenic microenvironment for cartilage regeneration.

3.9. GMOCS-exos facilitate the formation of cartilage matrix after growth plate injury

Having shown that GMOCS-Exos can create an anti-inflammatory microenvironment *in vivo*, we further investigated whether this microenvironment was conducive to the synthesis of cartilage matrix using COL-2 and MMP-13 IHC staining of the growth plate injury site. We found that the GMOCS group meaningfully boosted chondrocyte type 2 collagen expression while inhibiting chondrocyte MMP-13 expression compared with the control group, indicating that GMOCS hydrogel can promote chondrocytes anabolism rather than catabolism through the supplement of ECM directly. In addition, compared with the hydrogel treatment alone, Exo-loaded hydrogel further promoted the expression of COL-2, indicating that BMSCs-derived Exos can play a chondroprotective effect and promote cartilage regeneration. Combined with our finding in Fig. 7, we concluded that the local slow-release of Exos could inhibit the release of local inflammatory factors, relieve the inhibitory effect of the inflammatory environment on the cartilage gene SOX-9, and promote the expression of COL-2. It is essential to develop a scaffold material with good biocompatibility suitable for growth plate cartilage regeneration and the delivery of cells or various growth factors. In the last 20 years, research has mainly focused on tissue engineering scaffold materials combined with MSCs or growth factor transplantation to repair growth plate injury. For instance, David A. Puleo et al. used a

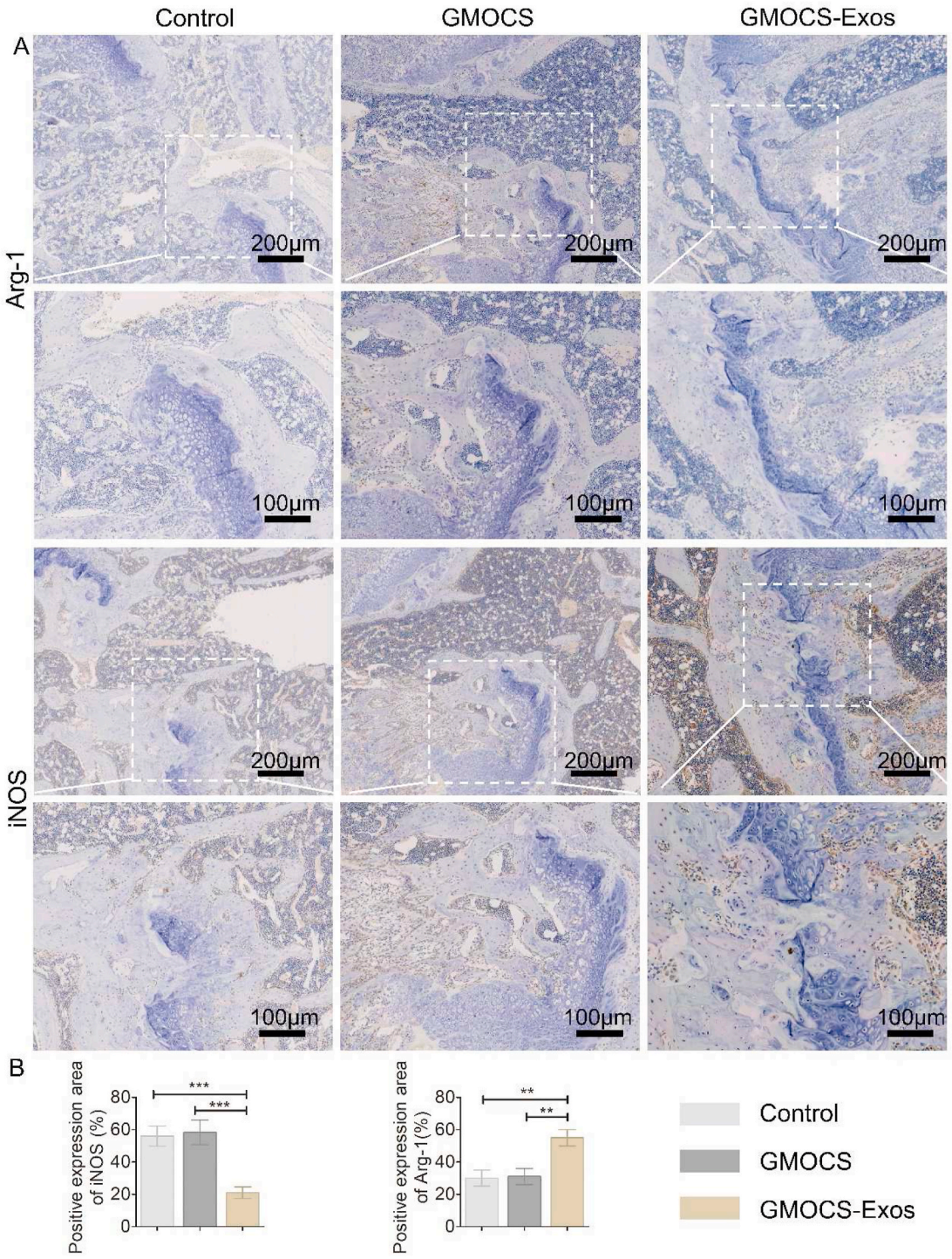

Fig. 7. Immunohistochemical staining and quantitative analysis of Arg-1 and iNOS protein at the defect site (n = 3). ANOVA followed by Tukey's test was used for statistical analysis (*p < 0.05, **p < 0.01, and ***p < 0.001).

poly (lactic-*co*-glycolic acid) (PLGA) scaffold to load insulin-like growth factor I (IGF-I) into the injury site and found that a small amount of cartilage tissue was formed [47]. Kiyoshi Yoshida et al. implanted synovial-derived mesenchymal stem cells combined with scaffold materials into the defect site of the rabbit growth plate and found that the formation of bone bridges was reduced [48]. In this study, our Exos loaded GMOCS hydrogels displayed excellent biocompatibility and anti-inflammatory properties beneficial to cartilage regeneration. Therefore more in-depth studies are warranted to provide new clinical therapeutic strategies in growth plate injuries repair in the future (see Fig. 8).

4. Conclusion

Herein, we developed a biocompatible GMOCS-Exos hydrogel composed of ECM and BMSCs-derived Exos to repair growth plate damage. Our GMOCS-Exos hydrogel regulated the balance of the ECM by promoting cartilage regeneration and reducing the inflammatory response. The results of *in vitro* and *in vivo* experiments show that GMOCS-Exos can exert anti-inflammatory effects through the slow release of Exos by regulating the polarization of M2 macrophages. Meanwhile, the anti-inflammatory effect of GMOCS-Exos can also improve the local microenvironment and promote the anabolism of

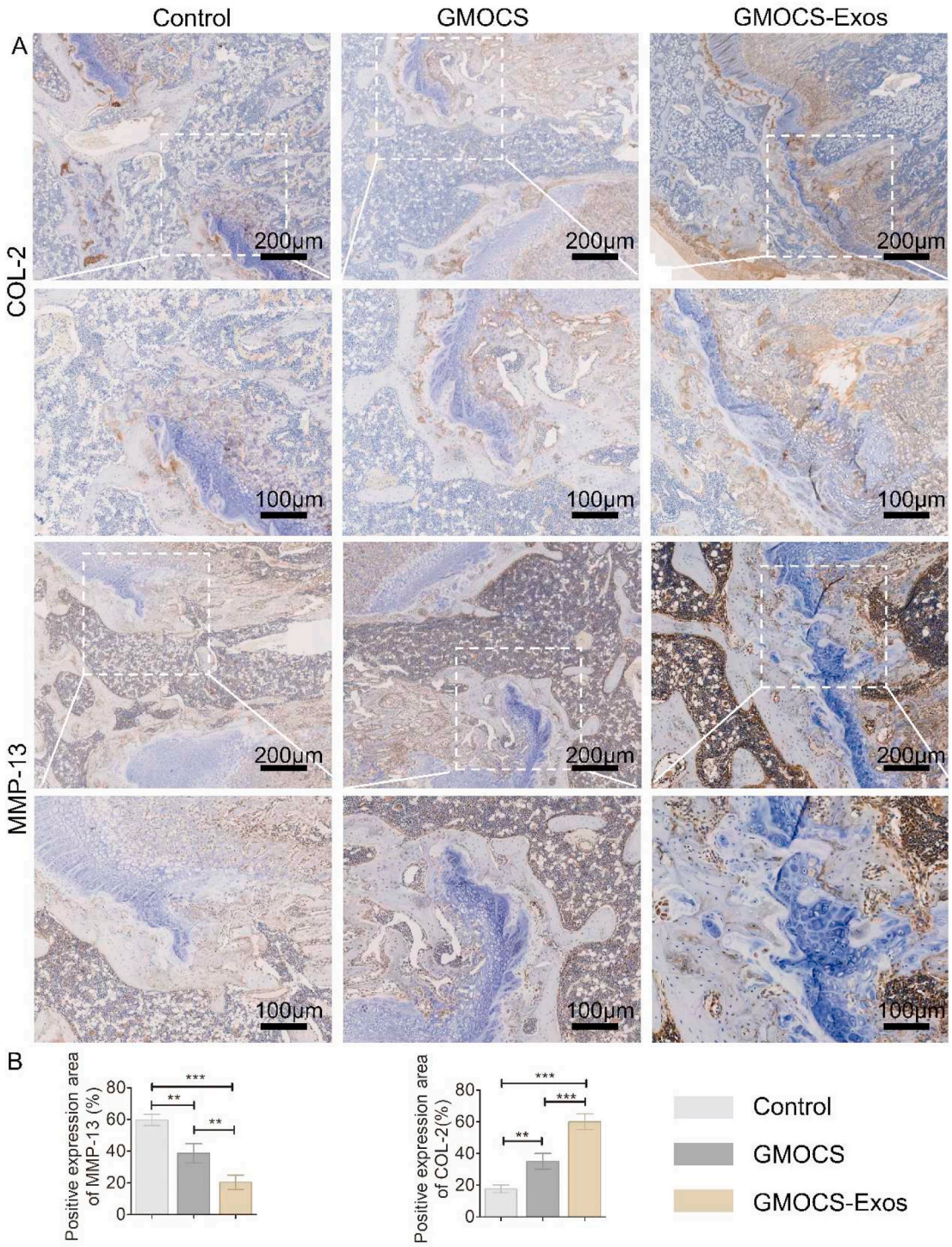

Fig. 8. Immunohistochemical staining and quantitative analysis of COL-2 and MMP-13 protein at the defect site (n = 3). ANOVA followed by Tukey's test was used for statistical analysis (*p < 0.05, **p < 0.01, and ***p < 0.001).

damaged chondrocytes, inhibiting bony repair after growth plate injury. Furthermore, GMOCS-Exos hydrogel can directly promote activity and ECM remodeling of chondrocytes. Therefore, our 3-dimensional Exo-loaded GMOCS hydrogel is a promising candidate for promoting cartilage regeneration after growth plate injury and reducing bone bridge formation.

CRediT authorship contribution statement

Pengfei Guan: Conceptualization, Methodology, Formal analysis, Validation, Writing – original draft. Can Liu: Conceptualization, Methodology, Investigation, Writing – review & editing. Denghui Xie: Methodology, Validation, Formal analysis. Shichao Mao: Methodology, Data curation. Yuelun Ji: Methodology, Data curation. Yongchang Lin: Methodology, Data curation. Zheng Chen: Methodology, Formal analysis. Qiyou Wang: Conceptualization, Validation, Resources,

Supervision. Lei Fan: Conceptualization, Methodology, Visualization, Supervision, Investigation, Formal analysis, Validation. Yongjian Sun: Conceptualization, Formal analysis, Supervision.

Declaration of competing interests

The authors declare that they have no known competing financial interests or personal relationships that could have appeared to influence the work reported in this paper.

Acknowledgments

We thank Lei Fan for his help in drawing the schematic diagram and typesetting figures. This study was supported by the Natural Science Foundation of Guangdong Province (No. 2020A1515011369).

Appendix A. Supplementary data

Supplementary data to this article can be found online at https://doi.org/10.1016/j.bioactmat.2021.09.010.

References

[1] C.E. Macsai, B. Hopwood, R. Chung, B.K. Foster, C.J. Xian, Structural and molecular analyses of bone bridge formation within the growth plate injury site and cartilage degeneration at the adjacent uninjured area, Bone 49 (4) (2011) 904–912.
[2] P.T. Newton, L. Li, B.Y. Zhou, C. Schweingruber, M. Hovorakova, M. Xie, X.Y. Sun, L. Sandhow, A.V. Artemov, E. Ivashkin, S. Suter, V. Dyachuk, M. El Shahawy, A. Gritli-Linde, T. Bouderlique, J. Petersen, A. Mollbrink, J. Lundeberg, G. Enikolopov, H. Qian, K. Fried, M. Kasper, E. Hedlund, I. Adameyko, L. Savendahl, A.S. Chagin, A radical switch in clonality reveals a stem cell niche in the epiphyseal growth plate, Nature 567 (7747) (2019) 234–+.
[3] C.B. Erickson, N. Shaw, N. Hadley-Miller, M.S. Riederer, M.D. Krebs, K.A. Payne, A rat tibial growth plate injury model to characterize repair mechanisms and evaluate growth plate regeneration strategies, Jove-J Vis Exp 125 (2017).
[4] D.J. Cepela, J.P. Tartaglione, T.P. Dooley, P.N. Patel, Classifications in brief: salter-harris classification of pediatric physeal fractures, Clin. Orthop. Relat. Res. 474 (11) (2016) 2531–2537.
[5] A.D. Theocharis, S.S. Skandalis, C. Gialeli, N.K. Karamanos, Extracellular matrix structure, Adv. Drug Deliv. Rev. 97 (2016) 4–27.
[6] J. Myllyharju, Extracellular matrix and developing growth plate, Curr. Osteoporos. Rep. 12 (4) (2014) 439–445.
[7] Y.W. Su, S.M. Chim, L. Zhou, M. Hassanshahi, R. Chung, C.M. Fan, Y.M. Song, B. K. Foster, C.A. Prestidge, Y. Peymanfar, Q. Tang, L.M. Butler, S. Gronthos, D. Chen, Y.L. Xie, L. Chen, X.F. Zhou, J.K. Xu, C.J. Xian, Osteoblast derived-neurotrophin-3 induces cartilage removal proteases and osteoclast-mediated function at injured growth plate in rats, Bone 116 (2018) 232–247.
[8] F.H. Zhou, B.K. Foster, G. Sander, C.J. Xian, Expression of proinflammatory cytokines and growth factors at the injured growth plate cartilage in young rats, Bone 35 (6) (2004) 1307–1315.
[9] S. Naahidi, M. Jafari, M. Logan, Y. Wang, Y. Yuan, H. Bae, B. Dixon, P. Chen, Biocompatibility of hydrogel-based scaffolds for tissue engineering applications, Biotechnol. Adv. 35 (5) (2017) 530–544.
[10] K. Yue, G. Trujillo-de Santiago, M.M. Alvarez, A. Tamayol, N. Annabi, A. Khademhosseini, Synthesis, properties, and biomedical applications of gelatin methacryloyl (GelMA) hydrogels, Biomaterials 73 (2015) 254–271.
[11] S. Li, F. Ma, X. Pang, B. Tang, L. Lin, Synthesis of chondroitin sulfate magnesium for osteoarthritis treatment, Carbohydr. Polym. 212 (2019) 387–394.
[12] M. Meghdadi, M. Pezeshki-Modaress, S. Irani, S.M. Atyabi, M. Zandi, Chondroitin sulfate immobilized PCL nanofibers enhance chondrogenic differentiation of mesenchymal stem cells, Int. J. Biol. Macromol. 136 (2019) 616–624.
[13] H. Liu, R.C. Li, T. Liu, L.Y. Yang, G. Yin, Q.B. Xie, Immunomodulatory effects of mesenchymal stem cells and mesenchymal stem cell-derived extracellular vesicles in rheumatoid arthritis, Front. Immunol. 11 (2020).
[14] M.B. Murphy, K. Moncivais, A.I. Caplan, Mesenchymal stem cells: environmentally responsive therapeutics for regenerative medicine, Exp. Mol. Med. 45 (2013).
[15] Y.F. Shi, Y. Wang, Q. Li, K.L. Liu, J.Q. Hou, C.S. Shao, Y. Wang, Immunoregulatory mechanisms of mesenchymal stem and stromal cells in inflammatory diseases, Nat. Rev. Nephrol. 14 (8) (2018) 493–507.
[16] D.H. Ha, H.K. Kim, J. Lee, H.H. Kwon, G.H. Park, S.H. Yang, J.Y. Jung, H. Choi, J. H. Lee, S. Sung, Y.W. Yi, B.S. Cho, Mesenchymal stem/stromal cell-derived exosomes for immunomodulatory therapeutics and skin regeneration, Cells-Basel 9 (5) (2020).
[17] C.R. Harrell, N. Jovicic, V. Djonov, N. Arsenijevic, V. Volarevic, Mesenchymal stem cell-derived exosomes and other extracellular vesicles as new remedies in the therapy of inflammatory diseases, Cells-Basel 8 (12) (2019).
[18] D.M. Pegtel, S.J. Gould, Exosomes, Annu. Rev. Biochem. 88 (2019) 487–514.
[19] R. Kalluri, V.S. LeBleu, The biology, function, and biomedical applications of exosomes, Science 367 (6478) (2020) 640–+.
[20] W.S. Toh, R.C. Lai, J.H.P. Hui, S.K. Lim, MSC exosome as a cell-free MSC therapy for cartilage regeneration: implications for osteoarthritis treatment, Semin. Cell Dev. Biol. 67 (2017) 56–64.
[21] N. Syn, L.Z. Wang, G. Sethi, J.P. Thiery, B.C. Goh, Exosome-Mediated metastasis: from epithelial-mesenchymal transition to escape from immunosurveillance, Trends Pharmacol. Sci. 37 (7) (2016) 606–617.
[22] L. Yin, Y.N. Wu, Z. Yang, V. Denslin, X.F. Ren, C.A. Tee, Z.X. Lai, C.T. Lim, J. Han, E.H. Lee, Characterization and application of size-sorted zonal chondrocytes for articular cartilage regeneration, Biomaterials 165 (2018) 66–78.
[23] L. Fan, P. Guan, C. Xiao, H. Wen, Q. Wang, C. Liu, Y. Luo, L. Ma, G. Tan, P. Yu, L. Zhou, C. Ning, Exosome-functionalized polyetheretherketone-based implant with immunomodulatory property for enhancing osseointegration, Bioact Mater 6 (9) (2021) 2754–2766.
[24] L. Li, Y. Zhang, J. Mu, J. Chen, C. Zhang, H. Cao, J. Gao, Transplantation of human mesenchymal stem-cell-derived exosomes immobilized in an adhesive hydrogel for effective treatment of spinal cord injury, Nano Lett. 20 (6) (2020) 4298–4305.
[25] L. Zhou, C. Dai, L. Fan, Y.H. Jiang, C. Liu, Z.N. Zhou, P.F. Guan, Y. Tian, J. Xing, X. J. Li, Y.A. Luo, P. Yu, C.Y. Ning, G.X. Tan, Injectable self-healing natural biopolymer-based hydrogel adhesive with thermoresponsive reversible adhesion for minimally invasive surgery, Adv. Funct. Mater. 31 (14) (2021).
[26] L.M. Li, Y. Zhang, J.F. Mu, J.C. Chen, C.Y. Zhang, H.C. Cao, J.Q. Gao, Transplantation of human mesenchymal stem-cell-derived exosomes immobilized in an adhesive hydrogel for effective treatment of spinal cord injury, Nano Lett. 20 (6) (2020) 4298–4305.
[27] R.M. Coleman, J.E. Phillips, A. Lin, Z. Schwartz, B.D. Boyan, R.E. Guldberg, Characterization of a small animal growth plate injury model using microcomputed tomography, Bone 46 (6) (2010) 1555–1563.
[28] S. Braune, R.A. Latour, M. Reinthaler, U. Landmesser, A. Lendlein, F. Jung, Vitro thrombogenicity testing of biomaterials, Adv Healthc Mater 8 (21) (2019).
[29] Y.P. Liang, X. Zhao, T.L. Hu, B.J. Chen, Z.H. Yin, P.X. Ma, B.L. Guo, Adhesive hemostatic conducting injectable composite hydrogels with sustained drug release and photothermal antibacterial activity to promote full-thickness skin regeneration during wound healing, Small 15 (12) (2019).
[30] K.A. Athanasiou, C. Zhu, D.R. Lanctot, C.M. Agrawal, X. Wang, Fundamentals of biomechanics in tissue engineering of bone, Tissue Eng. 6 (4) (2000) 361–381.
[31] R. Chung, C.J. Xian, Recent research on the growth plate: mechanisms for growth plate injury repair and potential cell-based therapies for regeneration, J. Mol. Endocrinol. 53 (1) (2014) T45–T61.
[32] S. Chen, W.M. Chen, Y.N. Chen, X.M. Mo, C.Y. Fan, Chondroitin sulfate modified 3D porous electrospun nanofiber scaffolds promote cartilage regeneration, Mat Sci Eng C-Mater 118 (2021).
[33] S.P. Zhang, S.J. Chuah, R.C. Lai, J.H.P. Hui, S.K. Lim, W.S. Toh, MSC exosomes mediate cartilage repair by enhancing proliferation, attenuating apoptosis and modulating immune reactivity, Biomaterials 156 (2018) 16–27.
[34] C. Wang, M. Wang, T. Xu, X. Zhang, C. Lin, W. Gao, H. Xu, B. Lei, C. Mao, Engineering bioactive self-healing antibacterial exosomes hydrogel for promoting chronic diabetic wound healing and complete skin regeneration, Theranostics 9 (1) (2019) 65–76.
[35] R. Kalluri, V.S. LeBleu, The biology, function, and biomedical applications of exosomes, Science 367 (6478) (2020).
[36] M. Fleshner, C.R. Crane, Exosomes, DAMPs and miRNA: features of stress physiology and immune homeostasis, Trends Immunol. 38 (10) (2017) 768–776.
[37] L. He, T. He, J. Xing, Q. Zhou, L. Fan, C. Liu, Y. Chen, D. Wu, Z. Tian, B. Liu, L. Rong, Bone marrow mesenchymal stem cell-derived exosomes protect cartilage damage and relieve knee osteoarthritis pain in a rat model of osteoarthritis, Stem Cell Res. Ther. 11 (1) (2020) 276.
[38] F.H. Zhou, B.K. Foster, G. Sander, C.J. Xian, Expression of proinflammatory cytokines and growth factors at the injured growth plate cartilage in young rats, Bone 35 (6) (2004) 1307–1315.
[39] S. Chen, W. Chen, Y. Chen, X. Mo, C. Fan, Chondroitin sulfate modified 3D porous electrospun nanofiber scaffolds promote cartilage regeneration, Mater Sci Eng C Mater Biol Appl 118 (2021) 111312.
[40] S. Zhang, K.Y.W. Teo, S.J. Chuah, R.C. Lai, S.K. Lim, W.S. Toh, MSC exosomes alleviate temporomandibular joint osteoarthritis by attenuating inflammation and restoring matrix homeostasis, Biomaterials 200 (2019) 35–47.
[41] E. Jimi, H. Fei, C. Nakatomi, NF-kappaB signaling regulates physiological and pathological chondrogenesis, Int. J. Mol. Sci. 20 (24) (2019).
[42] J. Melrose, C. Shu, J.M. Whitelock, M.S. Lord, The cartilage extracellular matrix as a transient developmental scaffold for growth plate maturation, Matrix Biol. 52–54 (2016) 363–383.
[43] T. Wirth, S. Byers, R.W. Byard, J.J. Hopwood, B.K. Foster, The implantation of cartilaginous and periosteal tissue into growth plate defects, Int. Orthop. 18 (4) (1994) 220–228.
[44] F.F. Sun, P.F. Hu, Y. Xiong, J.P. Bao, J. Qian, L.D. Wu, Tricetin protects rat chondrocytes against IL-1 beta-induced inflammation and apoptosis, Oxid Med Cell Longev (2019) 4695381, 2019.

[45] J. Lee, B. French, T. Morgan, S.W. French, The liver is populated by a broad spectrum of markers for macrophages. In alcoholic hepatitis the macrophages are M1 and M2, Exp. Mol. Pathol. 96 (1) (2014) 118–125.
[46] A. Stone, M.W. Grol, M.Z.C. Ruan, B. Dawson, Y.Q. Chen, M.M. Jiang, I.W. Song, P. Jayaram, R. Cela, F. Gannon, B.H.L. Lee, Combinatorial Prg4 and il-1ra gene therapy protects against hyperalgesia and cartilage degeneration in post-traumatic osteoarthritis, Hum. Gene Ther. 30 (2) (2019) 225–235.
[47] S.K. Sundararaj, R.D. Cieply, G. Gupta, T.A. Milbrandt, D.A. Puleo, Treatment of growth plate injury using IGF-I-loaded PLGA scaffolds, J Tissue Eng Regen Med 9 (12) (2015) E202–E209.
[48] K. Yoshida, C. Higuchi, A. Nakura, N. Nakamura, H. Yoshikawa, Treatment of partial growth arrest using an in vitro-generated scaffold-free tissue-engineered construct derived from rabbit synovial mesenchymal stem cells, J. Pediatr. Orthop. 32 (3) (2012) 314–321.